### Title

Targeted Quantitative Proteomics Revealed Arsenite-induced Proteasomal Degradation of RhoB in Fibroblast Cells.




### Journal

Chemical Research in Toxicology, 32(7)



### Authors

Tam, Lok
Huang, Ming
Wang, Yinsheng



### Publication Date

2019-07-15

### DOI

10.1021/acs.chemrestox.9b00155

Peer reviewed

HHS Public Access

Author manuscript

*Chem Res Toxicol*. Author manuscript; available in PMC 2020 July 15.

Published in final edited form as:

*Chem Res Toxicol*. 2019 July 15; 32(7): 1343–1350. doi:10.1021/acs.chemrestox.9b00155.

# Targeted Quantitative Proteomics Revealed Arsenite-induced Proteasomal Degradation of RhoB in Fibroblast Cells

**Lok Ming Tam**[†,§], **Ming Huang**[†,§], **Yinsheng Wang**[*,†,‡]

[†]Environmental Toxicology Graduate Program, University of California, Riverside, California 92521, United States

[‡]Department of Chemistry, University of California, Riverside, California 92521, United States

## Abstract

Arsenic is a toxicant widely present in the environment. Previous epidemiological and animal studies support that arsenic exposure is associated with elevated incidences of lung and skin cancers. Therefore, it is important to understand the molecular mechanisms through which arsenite initiates malignant transformation of lung and skin tissues. Ras superfamily of small GTPases assumes a crucial role in many cellular processes including transcription, protein synthesis, and trafficking. In addition, small GTPase signaling is known to be altered in many types of cancer. By employing a multiple-reaction monitoring (MRM)-based targeted proteomic method, we found that the protein level of RhoB was substantially decreased in IMR90 human lung fibroblast cells upon a 12-h exposure to 5 $\mu$M $NaAsO_2$. In addition, the protein level of ectopically expressed RhoB was found to decline in a dose-dependent manner upon arsenite exposure in HEK293T, HeLa, and GM00637 cells as well as that of endogenous RhoB protein in IMR90 cells. Moreover, the arsenite-elicited down-regulation of RhoB was found to arise from enhanced proteasomal degradation. Taken together, we demonstrated, for the first time, that exposure to arsenite could attenuate the protein expression of RhoB through proteasomal degradation.

## Graphical Abstract

[*]**Corresponding Author**: Yinsheng.Wang@ucr.edu. Phone: (951) 827-2700. Fax: (951) 827-4713.

[§]These authors contributed equally to this study.

Supporting Information

The Supporting Information is available free of charge on the ACS Publications website at DOI: 10.1021/acs.chemrestox.9b00155. Raw LC-MS/MS data for targeted analyses of small GTPase proteins in IMR90 cells upon a 12-hr exposure with 5 $\mu$M arsenite were deposited into PeptideAtlas with the identifier number of PASS01398. LC-MRM traces and Western blot images (PDF)

Quantication data of LC-MRM analysis reults (XLSX)

The authors declare no competing financial interest.

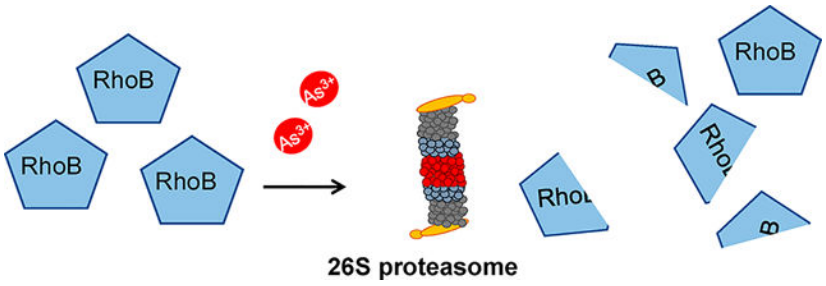


## INTRODUCTION

Arsenic, a naturally occurring element in the Earth's crust, has been recognized as the most detrimental metalloid existing prevalently in the environment, and arsenic exposure constitutes a major public health concern.[1,2] It was estimated that at least 150 million people in over 70 countries are exposed to excessive amount of arsenic species via contaminated drinking water and diet.[3] Arsenic has received substantial attention from the scientific community, and it is ranked on the top of the Priority List of Hazardous Substances in the Agency for Toxic Substances and Disease Registry (ATSDR).[4] Because of the tremendous public health burden from arsenic exposure through drinking water, the World Health Organization and the US Environmental Protection Agency (EPA) have set the maximum contamination level of arsenic in drinking water to be 10 ppb.[5,6] In addition, arsenic has been classified as a class I human carcinogen by the International Agency for Research on Cancer (IARC).

Chronic exposure to arsenic in drinking water was found to be associated with elevated incidences of various human diseases including bladder, lung, liver, skin, and kidney cancers.[7,8] Arsenic exists in both inorganic and organic forms.[9] However, arsenite, one of the major inorganic form of arsenic commonly detected in drinking water from the environment,[10] is found to show more potent toxicity toward humans than organic arsenic species.[11] Hence, it is critical and urgent to understand fully the molecular mechanisms underlying arsenite-induced carcinogenesis so as to develop suitable therapeutic and chemopreventive approaches.

Over the past few decades, small GTPases of the Ras superfamily have been widely studied and shown to be implicated in human cancers.[12,13] By shuffling between their GTP-bound active and GDP-bound inactive forms, small GTPases can serve as molecular switches in regulating a wide range of cellular processes including signal transduction, cell division, and cell motility.[14] Among them, Rho GTPases play important roles in controlling cell motility and cytoskeleton rearrangements, thereby regulating the architecture of stress fibers, focal adhesion, and membrane ruffles.[14] Additionally, a large number of studies demonstrated that Rho GTPases play regulatory roles in cancer cell migration and metastasis[13] and act as tumor suppressors or proto-oncogenes.[15] Furthermore, small Rho GTPases Rac1 and Cdc42 were previously found to be affected by arsenite exposure in rat nervous system.[16] We reason that a systematic study about how arsenite exposure modulates small GTPase signaling may provide new insights into the molecular mechanisms of arsenic toxicity and carcinogenicity.

Over the past two decades, mass spectrometry-based quantitative proteomics has become widely utilized to probe systematically the changes in protein expression and to study the signaling pathways involved in various human diseases.[17,18] Recently, several quantitative proteomic approaches have been developed and applied to study small GTPase proteins.[19−21]

In this study, we utilized our recently reported targeted quantitative proteomic method[21] for assessing the altered expression of small GTPases in cultured IMR90 human lung fibroblast cells upon arsenite treatment. We were able to quantify 87 small GTPases, among which RhoB exhibited the most pronounced down-regulation upon arsenite treatment. We also confirmed by Western blot analysis that exposure to arsenite leads to a dose-dependent decrease in the levels of both endogenous and ectopically expressed RhoB protein in cultured human cells and that the decreased protein levels of RhoB arise from its degradation by the 26S proteasome.

## EXPERIMENTAL PROCEDURES

### Cell Culture.

HEK293T human embryonic kidney epithelial cells (ATCC), HeLa human cervical cancer cells, and GM00637 human skin fibroblast cells were cultured in Dulbecco's modified Eagle's medium (DMEM, Thermo Fisher Scientific). IMR90 human lung fibroblast cells were cultured in Corning Eagle's minimum essential medium (EMEM, Thermo Fisher Scientific). All culture media except those used for transfection were supplemented with 10% fetal bovine serum (FBS, Thermo Fisher Scientific) and 1% penicillin–streptomycin solution (PS, GE Healthcare). The cells were maintained at 37 °C in a humidified atmosphere with 5% $CO_2$, with medium renewal in every 2–3 days depending on cell density. For plasmid transfection, the cells were cultured in the same media as described above except that no penicillin–streptomycin solution was added.

### Plasmid and Cell Transfection.

The expression plasmid for RhoB (pCMV3-HA-RhoB) was kindly provided by Dr. George Prendergast and Dr. Lisa Laury-Kleintop (Lankenau Institute for Medical Research).[22,23] The plasmid was transfected into GM00637, HEK293T, HeLa, and IMR90 cells using TransIT-2020 (Mirus Bio, Madison, WI) according to the manufacturer's recommended protocol.

### Western Blot Analysis.

IMR90, HEK293T, HeLa, and GM00637 cells were transfected with wild-type HA-RhoB. At 24 h after the transfection, the cells were exposed to different concentrations (i.e., 0, 1, 2, 5 $\mu$M) of $NaAsO_2$ for another 24 h and lysed in CelLytic M lysis buffer supplemented with a protease inhibitor cocktail (Sigma-Aldrich). For monitoring the expression of endogenous RhoB protein, untransfected IMR90 cells were exposed to the above-mentioned concentrations of $NaAsO_2$ for 24 h and lysed in the same way. After SDS-PAGE separation, proteins were transferred to a nitrocellulose membrane using a transfer buffer containing Tris base (25 mM, pH 8.1–8.5), methanol, glycine, and water. The membranes were blocked

with 5% BSA in PBS-T buffer, which contained PBS and 0.1% (v/v) Tween-20 (pH 7.5), for 1.5 h and incubated with rabbit anti-RhoB antibody (1:5000 dilution, Cell Signaling Technology) at room temperature for 2 h. The membranes were rinsed with fresh PBS-T at room temperature six times (5–10 min each). After being washed, the membranes were incubated with rabbit secondary antibody at room temperature for 1 h. The membranes were subsequently washed with PBS-T six times. The protein bands were detected using Amersham ECL Select Western blotting Detection Kit (GE Healthcare) and visualized with Hyblot CL autoradiography film (Denville Scientific, Inc., Metuchen, NJ).

To assess the effect of arsenite or MG132, a 26S proteasomal inhibitor, on the protein level of RhoB, HEK293T cells were transfected with HA-tagged RhoB plasmid for 24 h, and exposed with several different concentrations of $NaAsO_2$ (i.e., 0, 1, 2, and 5 $\mu$M) in the presence or absence of 4 $\mu$M MG132 (Sigma-Aldrich) for another 24 h, followed by cell harvesting, protein extraction, and Western blot analysis, as described above.

### Sample Preparation and LC-MRM Analysis.

For SILAC-based quantitative proteomics experiments, “heavy” and “light” SILAC DMEM media were freshly prepared by adding 0.146 g/L [$^{13}C_6$,$^{15}N_2$]-L-lysine (Lys-8) and 0.84 g/L [$^{13}C_6$]-L-arginine (Arg-6) (Cambridge Isotopes Inc.) or the corresponding unlabeled lysine (Lys-0) and arginine (Arg-0) to DMEM depleted of L-lysine and L-arginine (Thermo Scientific Pierce). The media were also supplemented with 10% dialyzed FBS (Corning) and 1% PS. IMR90 cells were cultured in the heavy-DMEM medium for at least 10 days or six cell doublings to enable complete heavy-isotope incorporation.

To assess the differential expression of small GTPases upon arsenite exposure, we conducted one forward and one reverse SILAC labeling experiment, where lysates of mock-treated light-labeled and arsenite (5 $\mu$M)-treated heavy-labeled IMR90 human lung fibroblast cells were combined at a 1:1 ratio (by mass) in the forward labeling experiment (Figure 1A). The reverse labeling experiment was conducted in the opposite way. The combined cell lysate (100 $\mu$g in total) was mixed with 4× Laemmli sample buffer (Bio-Rad) with 10% (v/v) 2-mercaptoethanol, boiled at 95 °C for 5 min, and then loaded and separated on a 10% SDS-PAGE gel at 120 V and at room temperature for 40 min. The gel band corresponding to the molecular weight range of 15–37 kDa was excised, and proteins in the gel slices were then reduced with 20 mM dithiothreitol, alkylated with 55 mM iodoacetamide, and digested in-gel with trypsin at an enzyme/protein ratio of 1:100 in 50 mM ammonium bicarbonate (pH 7.8) at 37 °C overnight. After tryptic digestion, the peptide mixtures were desalted and subjected to LC-MRM analyses.

All LC-MRM experiments were performed on a TSQ Vantage triple-quadrupole mass spectrometer (Thermo Scientific). The mass spectrometer was coupled with an EASY-nLC II system (Thermo Scientific), and the samples were automatically loaded onto a 4 cm trapping column (150 $\mu$m i.d.) packed with ReproSil-Pur 120 C18-AQ resin (5 $\mu$m in particle size and 120 Å in pore size, Dr. Maisch GmbH HPLC) at 3 $\mu$L/min. The trapping column was coupled to a 15 cm fused silica analytical column (75 $\mu$m i.d.) packed in-house with ReproSil-Pur 120 C18-AQ resin (3 $\mu$m in particle size and 120 Å in pore size, Dr. Maisch GmbH HPLC). The peptide mixtures were separated with a 157 min linear gradient of 2–

35% acetonitrile in 0.1% formic acid and at a flow rate of 230 nL/min. The spray voltage was 1.8 kV, Q1 and Q3 resolutions were 0.7 Da, and the cycle time was 5 s. The optimal collisional energy (CE) for each targeted peptide was calculated using a linear equation specific to the TSQ Vantage instrument and the precursor mass-to-charge ratio (m/z) according to the default setting in Skyline. A total of 432 peptides representing 113 nonredundant or 131 isoform-specific small GTPases were included in the library. The corresponding precursor and fragment ions of peptides harboring the light and heavy forms of lysine or arginine were monitored in two scheduled LC-MRM runs.

### Statistical Analysis.

The statistical analyses of all the Western blot experiments were performed by using the average of the values obtained from 3 to 4 independent experiments. The *p*-values used for all data analysis were calculated using unpaired two-tailed Student's *t*-test, which indicated the significant difference between the treated samples and the control with the asterisks as indicated (*, $0.01 \leq p < 0.05$; **, $0.001 \leq p < 0.01$; ***, $p < 0.001$).

## RESULTS

### Targeted Quantitative Profiling of Differential Expression of Small GTPases upon Arsenite Exposure in Lung Fibroblasts.

Lung constitutes a major target organ for arsenic-related carcinogenesis.[24] Given the crucial roles of small GTPases in cell signaling and trafficking related to various aspects of tumorigenesis and cancer progression,[25] we sought to investigate systematically the differential protein expression of small GTPases upon acute arsenite exposure in IMR90 human lung fibroblast cells. To this end, we employed a previously established targeted quantitative proteomics workflow, which involves SILAC, SDS-PAGE fractionation, and scheduled multiple-reaction monitoring (MRM) analysis (Figure 1A).[21]

To obtain reliable quantification results, we carried out the SILAC experiments in one set of forward labeling (Figure 1A) and one set of reverse labeling. In this vein, by adopting the scheduled MRM analysis, where the mass spectrometer is set up to monitor targeted transitions in a defined retention time window, high-throughput detection of peptides from small GTPases can be achieved. The entire library of small GTPase tryptic peptides could be monitored in two LC-MRM runs with retention time scheduling by using the iRT algorithm.[26]

The scheduled MRM analyses facilitated reproducible quantification of 87 small GTPases in both forward and reverse SILAC labeling experiments (Table S1 and Figure S1). By contrast, analysis of the same samples by LC–MS/MS in the data-dependent acquisition (DDA) mode only led to the identification of 36 and 39 small GTPases in the forward and reverse SILAC samples, respectively (Figure 1B). Moreover, MRM exhibited better sensitivity than the shotgun proteomic approach, as reflected by the substantially increased coverage of the small GTPase proteome in two one-dimensional LC-MRM runs (Figure 1B). We also examined the inter-replicate reproducibility of the MRM-based quantification. As illustrated in Figure 1C, the $Log_2$-transformed SILAC ratios for all the quantified small

GTPases obtained from forward and reverse SILAC labeling experiments are consistent, with a reasonably good linear fit ($R^2 = 0.824$). Taken together, the above results demonstrate that scheduled MRM analysis facilitates highly sensitive and reproducible quantitative profiling of perturbed expression of small GTPases in IMR90 cells upon acute arsenite exposure (5 $\mu$M, 12 h).

## Western Blot Analysis Validated Differential Expression of Small GTPases in IMR90 Cells upon Arsenite Exposure.

Among the 87 quantified small GTPases, RhoB exhibited the most pronounced attenuation at the protein level after arsenite exposure (Figure 1D). Hence, we decided to choose this protein for further study. We first conducted Western blot analyses of several small GTPases to confirm the relative protein expression levels of small GTPases in arsenite-treated over control cells observed from the targeted proteomic analysis. Our results showed that the protein expression levels of endogenous RhoB and ectopically expressed HA-RhoB were diminished substantially in IMR90 cells upon a 24 h exposure to 5 $\mu$M $NaAsO_2$, which is in line with the proteomic data (Figure 2B). Moreover, we examined the protein expression levels of two other small GTPases, Rab31 and Rab32, under the same exposure conditions. The Western blot analysis again confirmed the findings made from the proteomics experiment, where the protein expression levels of Rab31 and Rab32 remained unchanged upon arsenite exposure (Figure S1).

## Arsenite Exposure Led to Dose-Dependent Decrease in Expression Level of RhoB in IMR90, HEK293T, HeLa, and GM00637 Cells.

We next examined whether arsenite could induce a dose-dependent change in the expression level of RhoB. To this end, we exposed IMR90 cells with increasing concentrations (i.e., 0, 1, 2, and 5 $\mu$M) of $NaAsO_2$ for 24 h, and assessed the levels of endogenous RhoB by Western blot analysis. The Western blot result showed a dose-dependent decrease in the endogenous RhoB protein (Figure 3).

We also asked if this dose-dependent decrease in protein expression level of RhoB can be observed in other cell lines. Therefore, we exposed HEK293T cells, which were transfected with a plasmid for the ectopic expression of HA-RhoB, with increasing concentrations (i.e., 0, 1, 2, and 5 $\mu$M) of $NaAsO_2$ for 24 h and assessed the levels of HA-RhoB by Western blot analysis. Our results revealed a dose-dependent decrease in the level of RhoB protein (Figure 3). Similar findings were also made for HeLa human cervical cancer cells and GM00637 human skin fibroblast cells (Figure 3).

## Proteasomal Degradation Is Involved in Arsenite-Induced Decline in Protein Level of RhoB.

We also explored the mechanism through which arsenite induces the decrease in RhoB protein level by asking whether the ubiquitin-proteasome pathway is involved. To this end, we treated HA-RhoB-overexpressing HEK293T cells with 0, 2, or 5 $\mu$M of $NaAsO_2$ together with 4 $\mu$M MG132. As depicted in Figure 4, we found that MG132 treatment could augment the HA-RhoB protein level significantly when compared with the untreated control group. Importantly, the arsenite-induced decrease in HA-RhoB protein was largely rescued in cells

cotreated with MG132 (Figure 4). Thus, arsenite induces the decrease in HA-RhoB protein through promoting its degradation via the ubiquitin-proteasome pathway.

## DISCUSSION

### Targeted Quantitative Measurement of Small GTPases in Arsenite-Treated Lung Fibroblast Cells.

Increasing body of evidence from cellular, animal, and epidemiological studies support that small GTPases, particularly Rho GTPases, play critical roles in the initiation, progression, and metastatic transformation of human cancer.[12,13,27,28] Rho GTPases can serve as key molecular "switches" regulating cell motility, migration, invasion, and proliferation.[27,29] Moreover, arsenic is well-known for its carcinogenic effect.[6] Hence, we sought to investigate systematically the differential expression of small GTPases upon arsenite exposure, with the goal of gaining a mechanistic understanding about how arsenite exposure influences small GTPase signaling.

Our LC-MRM-based targeted quantitative proteomics method consistently detected the majority of small GTPases and revealed substantially changed expression of a number of small GTPases in IMR90 cells upon exposure to arsenite. Together with metabolic labeling by SILAC and fractionation by SDS-PAGE, the method facilitated unbiased and reproducible quantification of 87 small GTPases in arsenite-/vehicle-treated IMR90 cells. Compared to conventional DDA analysis, the MRM-based approach exhibits greater reproducibility, higher sensitivity, and increased throughput for the detection of small GTPases. We envision that this high-throughput and highly reliable method can be generally applicable for detecting and studying the protein expressions of small GTPases that are changed upon exposure to other environmental agents.

### Potential Roles of RhoB and Rabl5 in Arsenite-Induced Initiation of Malignant Transformation in Lung Fibroblast Cells.

Our targeted quantitative proteomics results showed that several small GTPases, including RhoB and Rabl5, have altered protein expression levels in IMR90 cells upon arsenite treatment. We further validated, by using Western blot analysis, that arsenite can induce the decrease in the levels of endogenous RhoB protein in IMR90 cells and ectopically expressed RhoB protein in IMR90, HEK293T, HeLa, and GM00637 cells (Figures 2 and 3). We also found that the arsenite-stimulated decrease of RhoB protein level in HEK293T cells involves the 26S proteasome.

During the early stage (i.e., initiation) of the arsenite-induced malignant transformation, cells begin to exhibit several hallmarks of cancer including enhanced cell proliferation and autonomous cell growth.[30,31] In addition, arsenic was found to perturb an array of signaling pathways including the PI3K/AKT pathway, which involves proteins that enhance cell growth, metabolism, survival, and proliferation.[24] Down-regulation of RhoB is known to promote the migration and invasion of human bronchial epithelial cells through activation of AKT1 and involvement of Rac1,[32] and also can induce Rac1-dependent epithelial-mesenchymal transition in lung cells through inhibition of PP2A.[33] Hence, our quantitative

proteomics data, together with previous findings, support the notion that arsenic may promote tumor progression, in part, by suppressing the RhoB-AKT-Rac1 pathway. Additionally, PI3K/AKT/mTOR pathway is commonly activated in non-small-cell lung cancer that constitutes more than 80% of worldwide lung cancer incidents.[34,35] Furthermore, RhoB is known to regulate negatively the migration and invasion of lung tissues through the AKT pathway.[36] However, the upstream target through which arsenic exposure induces the activation of PI3K/AKT/mTOR pathway remains unclear. Hence, our discovery of arsenic-induced proteasomal degradation of RhoB shed light on understanding how low-dose arsenic exposure could activate the PI3K/AKT/mTOR pathway, which is critical for lung oncogenesis.

It is worth noting that our quantitative proteomic experiment also led to observation of a markedly augmented expression of Rabl5 protein in IMR90 cells upon arsenite exposure (Figure 1D). Rabl5 protein was previously shown to be a component of the IFT-B complex responsible for anterograde ciliary protein traffcking in primary cilium.[37–39] Primary cilia function to sense diverse extracellular signals through a network of surface receptors on the ciliary membrane and play important roles in interpreting extracellular signals and regulating cell homeostasis by modulating different intracellular signaling pathways[37,38,40] including the Hedgehog signaling pathway in vertebrates.[37,39,40] Along this line, exposure to environmental arsenic could activate Hedgehog signaling, whose dysregulation may contribute to arsenic-induced tumorigenesis.[41] It will be important to investigate whether and how the arsenite-elicited up-regulation of Rabl5 protein contributes to arsenic toxicity and carcinogenicity.

## Implications in Environmental Exposure to Arsenic.

It is estimated that more than 150 million people in the world are exposed to inorganic arsenic in groundwater, in the concentration range of <1 ppb (mostly) to 5300 ppb (in certain regions).[3,42] In addition, multiple lines of evidence support that chronic exposure to low dose of arsenic species is strongly associated with malignancies including lung and skin cancers.[7,8,43–46] Therefore, it is imperative for us to understand comprehensively how long-term exposure to low levels of arsenite increase cell proliferation and hence augment the likelihood of the onset of malignant transformation. On the basis of the findings made from the present study, we propose that the onset of malignant transformation elicited by chronic, low-dose exposure to arsenic could be partly attributed to persistent induction of signaling pathways controlling cell cycle progression including the RhoB-Rac1 axis in PI3K/AKT signaling. In this context, it is worth noting that the present study was conducted under conditions of acute exposure of cultured human cells to a relatively high concentration of arsenite (5 $\mu$M). It will be important to examine, in the future, whether the findings made in the present study can be extended to chronic exposure to low doses of arsenic species. Last but not the least, growing body of literature supports the linkage between chronic arsenite exposure around the threshold concentration and the increased rates of arsenite-induced carcinogenesis in the exposed populations.[47] Therefore, US EPA should improve the current regulatory standard of arsenite in drinking water (10 ppb, which is equivalent to 77 nM) to safeguard the public health.

## Supplementary Material

Refer to Web version on PubMed Central for supplementary material.

## Funding

This research was supported by the National Institutes of Health (R01 ES025121 to Y.W.), and M.H. was supported in part by an NRSA T32 Institutional Training Grant (T32 ES018827).

## REFERENCES

(1). Argos M, Ahsan H, and Graziano JH (2012) Arsenic and human health: epidemiologic progress and public health implications. Rev. Environ. Health 27, 191–195. [PubMed: 22962196]

(2). Naujokas MF, Anderson B, Ahsan H, Aposhian HV, Graziano JH, Thompson C, and Suk WA (2013) The broad scope of health effects from chronic arsenic exposure: Update on a worldwide public health problem. Environ. Health Perspect 121, 295–302. [PubMed: 23458756]

(3). Chen SJ, Zhou GB, Zhang XW, Mao JH, De Thé H, and Chen Z (2011) From an old remedy to a magic bullet: Molecular mechanisms underlying the therapeutic effects of arsenic in fighting leukemia. Blood 117, 6425–6437. [PubMed: 21422471]

(4). Bissen M, and Frimmel FH (2003) Arsenic − A Review. Part I: Occurrence, Toxicity, Speciation, Mobility. Acta Hydrochim. Hydrobiol 31, 9–18.

(5). Hughes MF (2002) Arsenic toxicity and potential mechanisms of action. Toxicol. Lett 133, 1–16. [PubMed: 12076506]

(6). Ravenscroft P, Brammer H, and Richards K (2009) Arsenic Pollution: A Global Synthesis, Wiley-Blackwell, UK.

(7). Shen S, Li X, Cullen WR, Weinfeld M, and Le XC (2013) Arsenic Binding to Proteins. Chem. Rev 113, 1–48. [PubMed: 23039127]

(8). Kumar A, Adak P, Gurian PL, and Lockwood JR (2010) Arsenic exposure in US public and domestic drinking water supplies: A comparative risk assessment. J. Exposure Sci. Environ. Epidemiol 20, 245–254.

(9). Martinez VD, Vucic EA, Becker-Santos DD, Gil L, and Lam WL (2011) Arsenic exposure and the induction of human cancers. J. Toxicol 2011, 431287. [PubMed: 22174709]

(10). Hartwig A, Blessing H, Schwerdtle T, and Walter I (2003) Modulation of DNA repair processes by arsenic and selenium compounds. Toxicology 193, 161–167. [PubMed: 14599775]

(11). Arita A, and Costa M (2009) Epigenetics in metal carcinogenesis: Nickel, Arsenic, Chromium and Cadmium. Metal-lomics 1, 222–228.

(12). Porter AP, Papaioannou A, and Malliri A (2016) Deregulation of Rho GTPases in cancer. Small GTPases 7, 123–138. [PubMed: 27104658]

(13). Alan JK, and Lundquist EA (2013) Mutationally activated Rho GTPases in cancer. Small GTPases 4, 159–163. [PubMed: 24088985]

(14). Delprato A (2012) Topological and Functional Properties of the Small GTPases Protein Interaction Network. PLoS One 7, No. e44882.

(15). Zandvakili I, Lin Y, Morris JC, and Zheng Y (2017) Rho GTPases: Anti- or Pro-neoplastic Targets? Oncogene 36, 3213–3222. [PubMed: 27991930]

(16). Heck AJ, and Krijgsveld J (2004) Mass spectrometry-based quantitative proteomics. Expert Rev. Proteomics 1, 317–326. [PubMed: 15966828]

(17). Aebersold R, and Mann M (2003) Mass spectrometry-based proteomics. Nature 537, 347–355.

(18). Zhang CC, Li R, Jiang H, Lin S, Rogalski JC, Liu K, and Kast J (2015) Development and application of a quantitative multiplexed small GTPase activity assay using targeted proteomics. J. Proteome Res 14, 967–976. [PubMed: 25569337]

(19). Marelli M, Smith JJ, Jung S, Yi E, Nesvizhskii AI, Christmas RH, Saleem RA, Tam YYC, Fagarasanu A, Goodlett DR, Aebersold R, Rachubinski RA, and Aitchison JD (2004)

Quantitative mass spectrometry reveals a role for the GTPase Rho 1 p in actin organization on the peroxisome membrane. J. Cell Biol 167, 1099–1112. [PubMed: 15596542]

(20). Huang M, Qi TF, Li L, Zhang G, and Wang Y (2018) A targeted quantitative proteomic approach assesses the reprogramming of small GTPases during melanoma metastasis. Cancer Res. 78, 5431–5445. [PubMed: 30072397]

(21). Lebowitz P, Davide J, and Prendergast GC (1995) Evidence that farnesyltransferase inhibitors suppress Ras transformation by interfering with Rho activity. Mol. Cell. Biol 15, 6613–6622. [PubMed: 8524226]

(22). Mandik-Nayak L, DuHadaway JB, Mulgrew J, Pigott E, Manley K, Sedano S, Prendergast GC, and Laury-Kleintop LD (2017) RhoB blockade selectively inhibits autoantibody production in autoimmune models of rheumatoid arthritis and lupus. Dis. Models & Mech 10, 1313–1322.

(23). An Y, Liu T, Liu X, Zhao L, and Wang J (2016) Rac1 and Cdc42 Play Important Roles in Arsenic Neurotoxicity in Primary Cultured Rat Cerebellar Astrocytes. Biol. Trace Elem. Res 170, 173–82. [PubMed: 26231544]

(24). Hubaux R, Becker-Santos DD, Enfield KS, Rowbotham D, Lam S, Lam WL, and Martinez VD (2013) Molecular features in arsenic-induced lung tumors. Mol. Cancer 12, 20. [PubMed: 23510327]

(25). Prieto-Dominguez N, Parnell C, and Teng Y (2019) Drugging the Small GTPase Pathways in Cancer Treatment: Promises and Challenges. Cells 8, 255.

(26). Escher C, Reiter L, MacLean B, Ossola R, Herzog F, Chilton J, MacCoss MJ, and Rinner O (2012) Using iRT, a normalized retention time for more targeted measurement of peptides. Proteomics 12, 1111–1121. [PubMed: 22577012]

(27). Haga RB, and Ridley AJ (2016) Rho GTPases: Regulation and roles in cancer cell biology. Small GTPases 7, 207–221. [PubMed: 27628050]

(28). Kazanietz MG, and Caloca MJ (2017) The Rac GTPase in cancer: From old concepts to new paradigms. Cancer Res. 77, 5445–5451. [PubMed: 28807941]

(29). Cardama GA, Gonzalez N, Maggio J, Lorenzano Menna P, and Gomez DE (2017) Rho GTPases as therapeutic targets in cancer. Int. J. Oncol 51, 1025–1034. [PubMed: 28848995]

(30). Hanahan D, and Weinberg RA (2000) The hallmarks of cancer. Cell 100, 57–70. [PubMed: 10647931]

(31). Cooper GM (2000) The Cell: A Molecular Approach, 2nd ed., Sinauer Associates, Sunderland, MA.

(32). Bousquet E, Mazières J, Privat M, Rizzati V, Casanova A, Ledoux A, Mery E, Coudere B, Gavre G, and Pradines A (2009) Loss of RhoB expression promotes migration and invasion of human bronchial cells via activation of AKT1. Cancer Res. 69, 6092–6099. [PubMed: 19602596]

(33). Bousquet E, Calvayrac O, Mazières J, Lajoie-Mazenc I, Boubekeur N, Favre G, and Pradines A (2016) RhoB loss induces Rac1-dependent mesenchymal cell invasion in lung cells through PP2A inhibition. Oncogene 35, 1760–1769. [PubMed: 26148238]

(34). Cheng H, Shcherba M, Pendurti G, Liang Y, Piperdi B, and Perez-Soler R (2014) Targeting the PI3K/AKT/mTOR pathway: potential for lung cancer treatment. Lung Cancer Manage. 3, 67–75.

(35). Pérez-Ramírez C, Cañadas-Garre M, Molina MÁ¸ Faus-Dáder MJ, and Calleja-Hernández MÁ (2015) PTEN and PI3K/AKT in non-small-cell lung cancer. Pharmacogenomics 16, 1843–1862. [PubMed: 26555006] ¸

(36). Jiang K, Sun J, Cheng J, Djeu JY, Wei S, and Sebti S (2004) Akt mediates Ras downregulation of RhoB, a suppressor of transformation, invasion, and metastasis. Mol. Cell. Biol 24, 5565–5576. [PubMed: 15169915]

(37). Ávalos Y, Peña-Oyarzun D, Budini M, Morselli E, and Criollo A (2017) New Roles of the Primary Cilium in Autophagy. BioMed Res. Int. 2017, 1.

(38). Yuan X, Serra RA, and Yang S (2015) Function and regulation of primary cilia and intraflagellar transport proteins in the skeleton. Ann. N. Y. Acad. Sci 1335, 78–99. [PubMed: 24961486]

(39). Lechtreck KF (2015) IFT-cargo interactions and protein transport in cilia. Trends Biochem. Sci 40, 765–778. [PubMed: 26498262]

(40). Wang L, and Dynlacht BD (2018) The regulation of cilium assembly and disassembly in development and disease. Development 145, No. dev151407.

(41). Fei DL, Li H, Kozul CD, Black KE, Singh S, Gosse JA, DiRenzo J, Martin KA, Wang B, Hamilton JW, Karagas MR, and Robbins DJ (2010) Activation of Hedgehog signaling by the environmental toxicant arsenic may contribute to the etiology of arsenic induced tumors. Cancer Res. 70, 1981–1988. [PubMed: 20179202]

(42). Smedley PL, and Kinniburgh DG (2000) Source and behaviour of arsenic in natural waters. Br. Geol. Surv 2000, 61.

(43). Person RJ, Ngalame NNO, Makia NL, Bell MW, Waalkes MP, and Tokar EJ (2015) Chronic inorganic arsenic exposure in vitro induces a cancer cell phenotype in human peripheral lung epithelial cells. Toxicol. Appl. Pharmacol 286, 36–43. [PubMed: 25804888]

(44). Stueckle TA, Lu Y, Davis ME, Wang L, Jiang B, Holaskova I, Schafer R, Barnette JB, and Rojanasakui Y (2012) Chronic occupational exposure to arsenic induces carcinogenic gene signaling networks and neoplastic transformation in human lung epithelial cells. Toxicol. Appl. Pharmacol 261, 204–216. [PubMed: 22521957]

(45). Yoshida T, Yamauchi H, and Sun GF (2004) Chronic health effects in people exposed to arsenic via the drinking water: Dose-response relationships in review. Toxicol. Appl. Pharmacol 198, 243–252. [PubMed: 15276403]

(46). Reichard JF, Schnekenburger M, and Puga A (2007) Long term low-dose arsenic exposure induces loss of DNA methylation. Biochem. Biophys. Res. Commun 352, 188–192. [PubMed: 17107663]

(47). Schmidt CW (2014) Low-dose arsenic in search of a risk threshold. Environ. Health Perspect 122, 130–134.

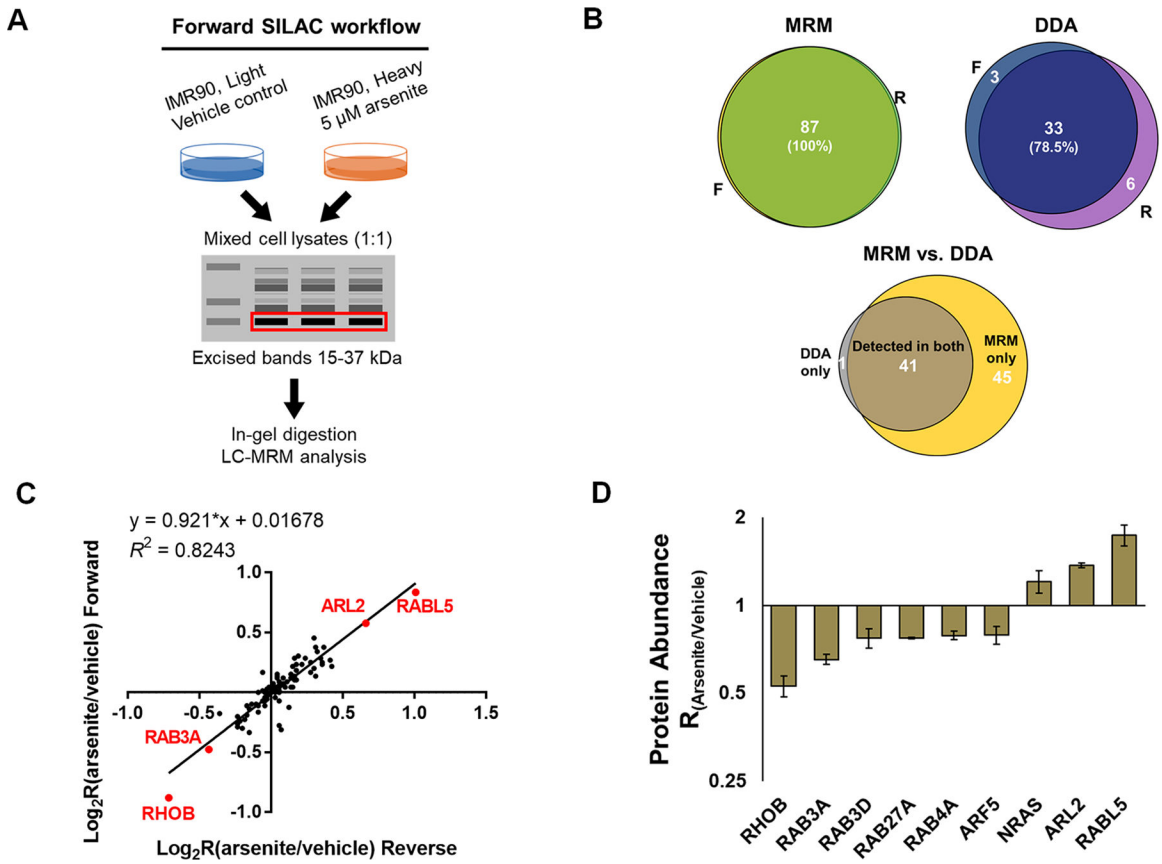


**Figure 1.**

Targeted proteomic strategy for high-throughput quantitative profiling of small GTPases upon arsenite exposure in IMR90 human lung fibroblast cells. (A) Schematic illustration of the targeted quantitative proteomic workflow, relying on forward SILAC labeling, SDS-PAGE fractionation, and scheduled LC-MRM analysis; (B) Venn diagrams displaying the overlap between quantified small GTPases in the forward and reverse SILAC experiments obtained from the MRM and DDA analyses, respectively, and the comparison between the performances of the two methods; (C) correlation between the $Log_2$-transformed SILAC ratios ($Log_2R$) obtained from one forward and one reverse SILAC labeling experiments with a relatively high linear correlation coefficient ($R^2$ = 0.8243); (D) bar chart showing significantly up- and down-regulated (>1.5-fold) small GTPases quantified from two LC-MRM experiments.

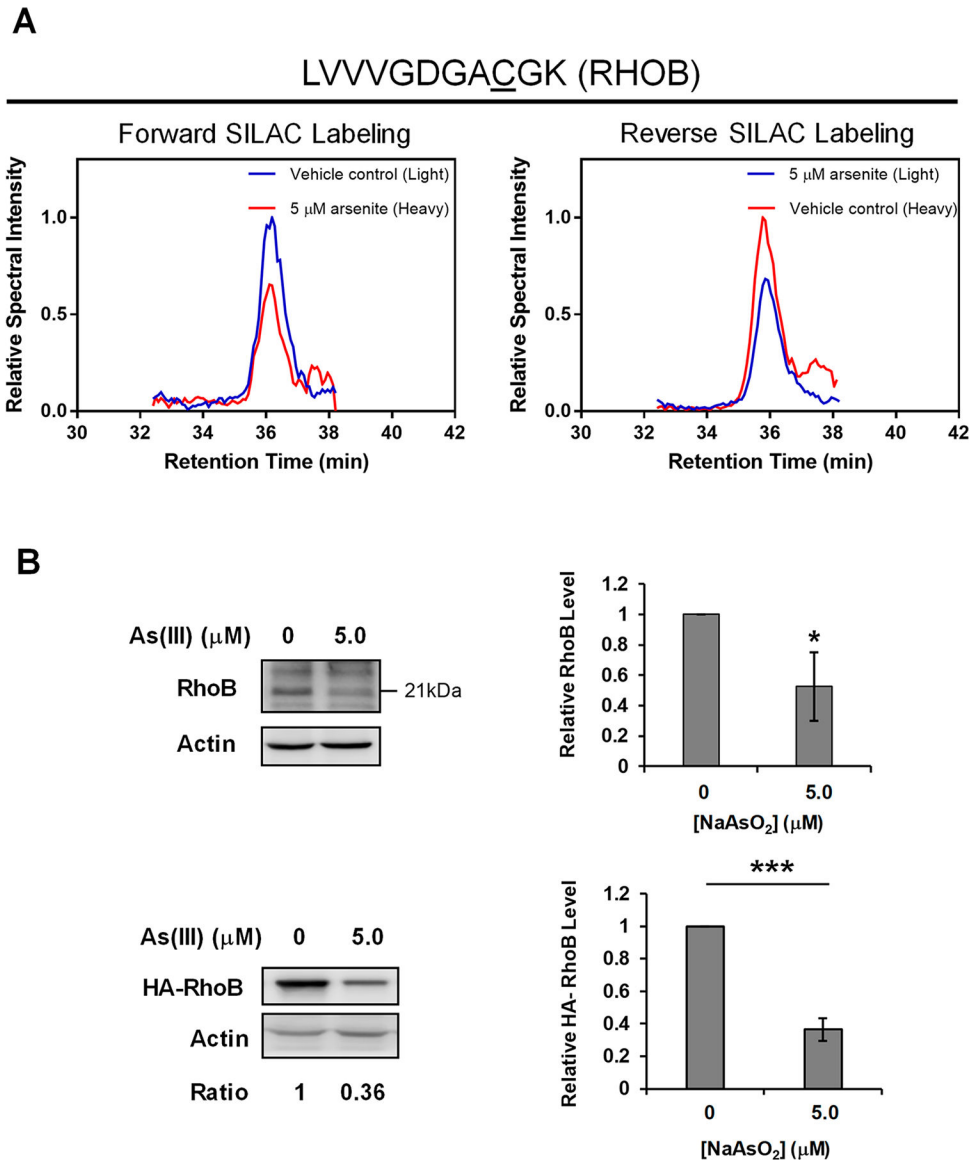


**Figure 2.**

LC-MRM and Western blot analyses revealed consistently lower levels of expression of RhoB upon a 12 h exposure to 5 $\mu$M $NaAsO_2$ in IMR90 cells. (A) Extracted MRM traces for three transitions ($y_9$, $y_8$, and $y_7$) monitored for the $[M+2H]^{2+}$ ion ($m/z$ 537.78) of a tryptic peptide from RhoB, that is, LVVVGDGACGK (underlined 'C' designates carbamidomethylated Cys), with blue and red traces representing MRM transitions for the light- and heavy-isotope labeled forms of the peptide, respectively; (B) Western blot analysis confirmed the diminished expression of both endogenous and ectopically expressed RhoB in IMR90 cells upon exposure to 5 $\mu$M of $NaAsO_2$ for 24 h. Shown are the quantification results for the relative levels of RhoB protein following exposure to 5 $\mu$M of $NaAsO_2$ obtained from Western blot analysis. Error bars represent standard deviations ($n$ = 3). The $p$-values were calculated using unpaired two-tailed student's $t$-test, and the asterisks designate

significant differences between arsenite-treated samples and untreated control (*, $0.01 \leq p < 0.05$; **, $0.001 \leq p < 0.01$; ***, $p < 0.001$).

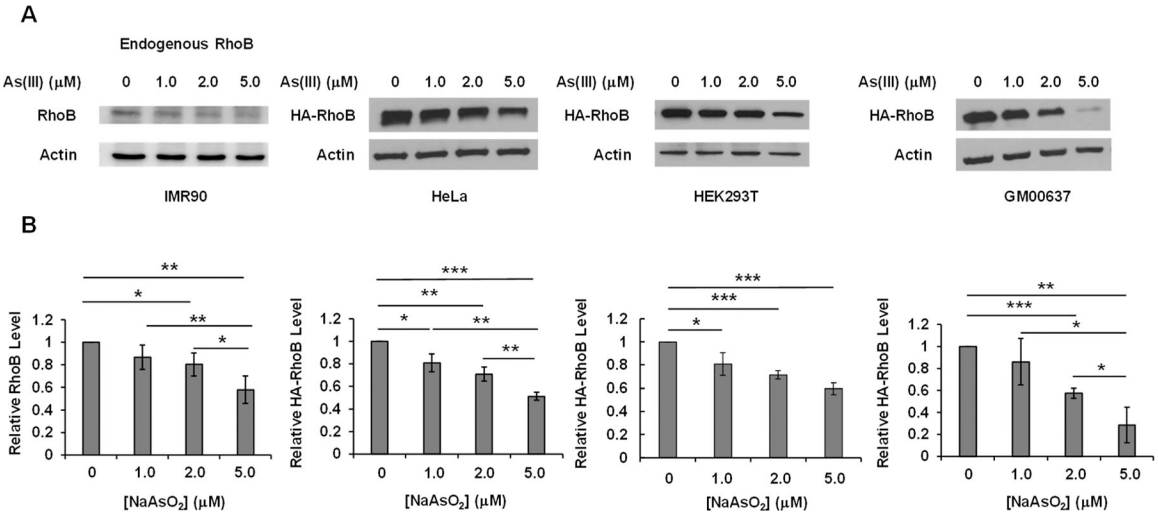


**Figure 3.**

Arsenite treatment results in a dose-dependent decrease in both endogenous and ectopically expressed RhoB proteins. (A) Western blot images showing the effect of 24 h treatment with different doses of arsenite (0, 1, 2, and 5 $\mu$M) on expression level of endogenous RhoB protein in IMR90 cells and ectopically expressed HA-RhoB protein in HeLa, HEK293T and GM00637 cells. (B) Quantification results of the relative levels of endogenous and ectopically expressed RhoB protein in the four cell lines as shown in panel A following exposure to different doses of $NaAsO_2$. Error bars represent standard deviations ($n = 3$). The $p$-values were calculated using unpaired two-tailed student's $t$-test, and the asterisks designate significant differences between arsenite-treated samples and untreated control (*, $0.01 \leq p < 0.05$; **, $0.001 \leq p < 0.01$; ***, $p < 0.001$).

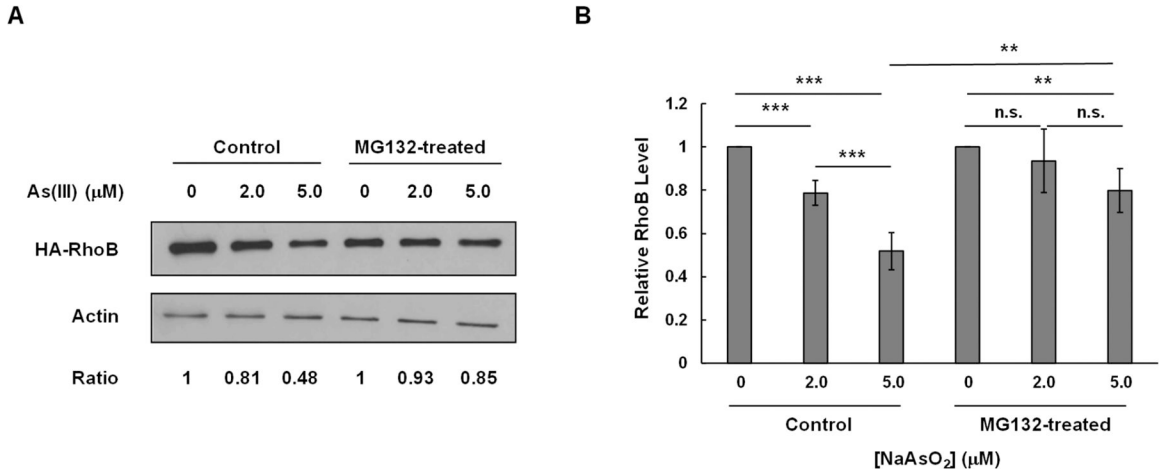


**Figure 4.**

Exposure to arsenite induces proteasomal degradation of RhoB. (A) Co-treatment of HEK293T cells with 4 $\mu$M MG132 together with different doses of $NaAsO_2$ (0, 2, and 5 $\mu$M) for 24 h could rescue the dose-dependent decrease of RhoB protein induced by arsenite exposure. (B) Relative protein level of HA-RhoB upon treatment with different doses of $NaAsO_2$ together with MG132 or DMSO control ($n = 3$). The $p$-values were calculated using unpaired two-tailed student's $t$-test, and the asterisks designate significant differences between the arsenite-treated samples and untreated control (*, $0.01 \leq p < 0.05$; **, $0.001 \leq p < 0.01$; ***, $p < 0.001$). n.s. represents no significant difference between arsenite-treated samples and untreated control.